14th International Symposium on Turbulence and Shear Flow Phenomena (TSFP14)
Heidelberg, Germany, July 28–31, 2026

DIRECT LAGRANGIAN SIMULATION OF DROPLET GROWTH IN A VERTICALLY DEVELOPING TURBULENT CLOUD

Masaya Iwashima
Department of Mechanical Engineering
Institute of Science Tokyo
2-12-1 Ookayama, Meguro-ku, Tokyo 152-8550 Japan
iwashima.m.6147@m.isct.ac.jp

Ryo Onishi
Supercomputing Research Center
Institute of Science Tokyo
2-12-1 Ookayama, Meguro-ku, Tokyo 152-8550 Japan
onishi.ryo@scrc.iir.isct.ac.jp

ABSTRACT

A new explicit warm-cloud microphysical model based on direct numerical simulation (DNS) with Lagrangian particle tracking is presented. The novelty of the model lies in the adoption of a vertically-elongated quasi one-dimensional computational domain covering the whole cloud layer. This framework enables us to capture the vertical structure of the cloud and represent all warm-cloud microphysics processes. Using this new model, we performed two cases of simulations, with and without turbulent velocity fluctuations. We analyzed the statistics of droplet collisions to quantitatively evaluate the effects of turbulence. The results clarified large impacts of turbulence on cloud microphysics. At the early developing stage with non-zero vertical velocity, droplet collisions with similar sizes (autoconversions) were promoted in the inner cloud with turbulence. The promoted autoconversions led to the active collections of small droplets by relatively large droplets (accretions). The turbulence also affected the growth history of raindrops reaching the ground surface.

INTRODUCTION

Turbulence plays an important role for cloud microphysics (Vaillancourt & Yau, 2000). Since 1990s, direct numerical simulation (DNS) with Lagrangian particle tracking has been utilized to investigate the effects of turbulence on cloud microphysics. In Woittiez et al. (2009), they investigated the effects of turbulence and gravity on the collision statistics of cloud droplets. In Onishi et al. (2015), they focused on the collision-coalescence growth of cloud droplets in turbulence. Saito & Gotoh (2018) included the effects of condensation/evaporation growth in addition to the collision-coalescence growth in DNS.

In these studies, a cubic domain with periodic boundary conditions (periodic box domain) is used. Although the periodic box domain is easy to handle numerically, it is not physically realistic. In the real atmospheric cloud, there are vertical structures in terms of e.g. water vapor mixing ratio or droplet size distribution. However, in the periodic box domain, it is difficult to represent these vertical structures.

In Kunishima & Onishi (2018), they proposed a new approach to overcome this limitation. They adopted a vertically-elongated quasi one-dimensional computational domain covering from the cloud top to the ground. This vertically-elongated domain could capture the vertical structure of the cloud in the Lagrangian particle tracking simulation. Due to this setting, they could simulate all warm-cloud microphysical processes, which are cloud condensation nuclei (CCN) activation, condensation/evaporation growth, collision-coalescence growth, and gravitational settling. However, they did not consider the effects of turbulence on cloud microphysics.

In this study, we developed a new numerical model of cloud microphysics based on DNS with Lagrangian particle tracking. The aim is to capture the effects of turbulence on all cloud microphysics processes explicitly. Using the vertically-elongated quasi one-dimensional computational domain with homogeneous isotropic turbulence field, we investigate the effects of turbulence.

NUMERICAL SIMULATION

Overview

The numerical simulation is based on Lagrangian Cloud Simulator (LCS) (Onishi et al., 2015), which is a DNS-based cloud microphysical simulation with Lagrangian particle tracking. In LCS, the flow and the scalar fields are computed on the Eulerian grid, while the precipitation particles are tracked in the Lagrangian way.

LCS with vertically-elongated domain is based on Kunishima & Onishi (2018). Figure 1 shows the schematic image of the cloud microphysical simulation in the vertically-elongated domain. In the simulation, we consider the all warm-cloud microphysical processes,

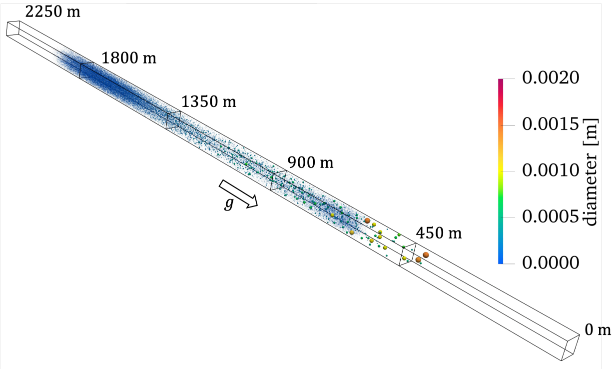

Figure 1: Schematic image of Lagrangian tracking cloud microphysics simulation in a vertically-elongated quasi one-dimensional computational domain.

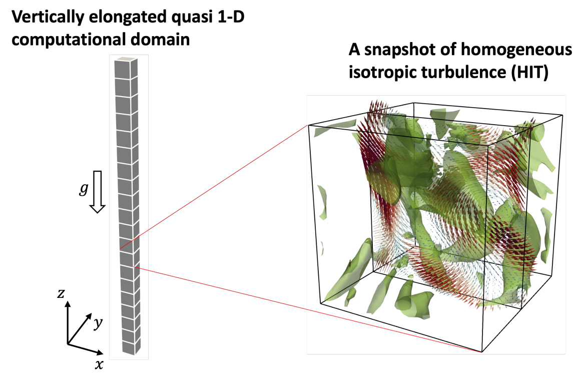

Figure 2: A snapshot of homogeneous isotropic turbulence (HIT) is implemented by stacking periodically in the vertical direction in the domain.

Table 1: Computational settings and statistics obtained in a statistically steady state of homogeneous isotropic turbulence (HIT) .

Number of grids N [−]	Domain size L_x [m]	Kolmogorov scale η [m]	Energy dissipation rate ε [m^2 s^{-3}]
32	5.00×10^{-3}	4.27×10^{-4}	1.01×10^{-1}

Table 2: Initial profile for KiD warm1 case in Shipway & Hill (2012).

Altitude z [m]	Potential temperature Θ [K]	Water vapor mixing ratio Q_v [kg kg^{-1}]
2250	306.7	0.00697
740	297.9	0.0138
0	297.9	0.0150

Table 3: Computational settings for two cases of simulations.

	LAM-case	TURB-case
Grid size of fluid computation $\Delta x^2 \times \Delta z$	$(1.67 \times 10^{-3}) \times (9.77 \times 10^{-3})$	$(3.125 \times 10^{-4}) \times (3.125 \times 10^{-4})$
Time interval Δt [s]	1.25×10^{-3}	5.00×10^{-5}

which are CCN activation, condensation/evaporation growth, collision-coalescence growth, and gravitational settling.

In order to capture the effect of turbulence on the cloud microphysics, a snapshot of homogeneous isotropic turbulence (HIT) is incorporated into the vertically-elongated domain. The HIT snapshot is periodically stacked in the vertical direction within the domain. Figure 2 shows the schematic image of the implementation of the HIT snapshot in the vertically-elongated domain.

Profiles of homogeneous isotropic turbulence

Table 1 shows the computational settings and statistics of the obtained HIT snapshot. The size of the snapshot L_x [m] is equal to the horizontal size of the vertically-elongated domain. The energy dissipation

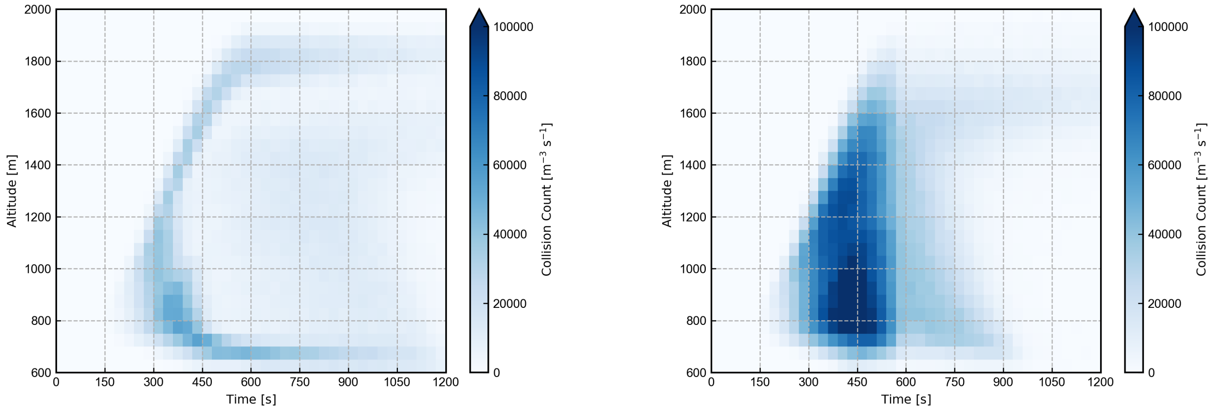

(a) LAM-case. (b) TURB-case.

Figure 3: Collision frequency $[\mathrm{m^{-3}s^{-1}}]$ of droplet pairs with the diameter ratio between 1 and 2.

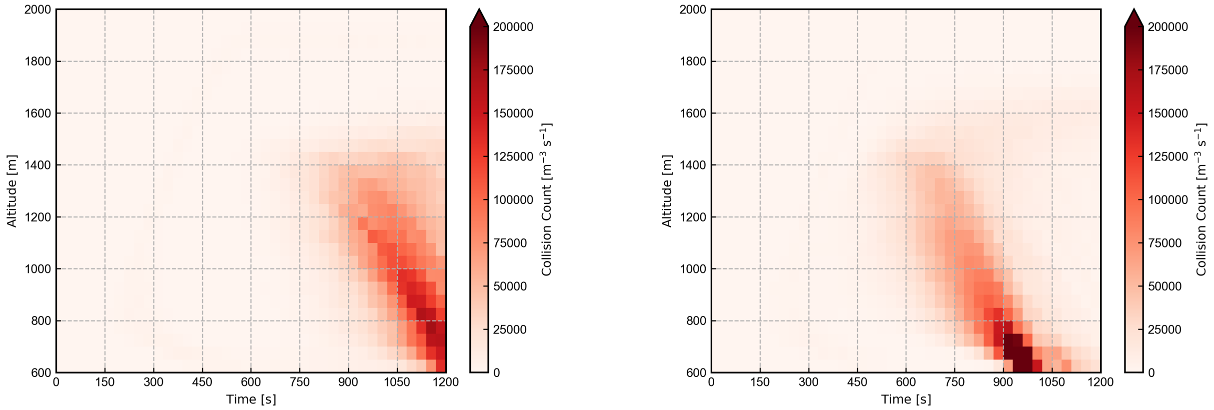

(a) LAM-case. (b) TURB-case.

Figure 4: Collision frequency $[\mathrm{m^{-3}s^{-1}}]$ of droplet pairs with the diameter ratio of 2 or greater.

rate ε $[\mathrm{m^2\ s^{-3}}]$ is set so that cumulus or cumulonimbus clouds ($\varepsilon \sim 10^{-2}$–10^{-1} $\mathrm{m^2\ s^{-3}}$) are assumed.

Kinematic model

In this study, a kinematic model is adopted. The kinematic model is used in meteorological simulations in which the flow field is prescribed. In our simulations, the warm-1 case in Kinematic Driver (KiD warm1) (Shipway & Hill, 2012) is adopted.

In the KiD warm1, the simple updraft is prescribed in the first 600 s described in the equation below.

$$w_{\mathrm{updraft}} = \begin{cases} w_0 \sin\left(\frac{\pi t}{600}\right) & (0\ \mathrm{s} \leq t < 600\ \mathrm{s}) \\ 0 & (600\ \mathrm{s} \leq t) \end{cases}, \quad (1)$$

where $w_0 = 2\ \mathrm{m\ s^{-1}}$. In the present paper, the period of the first 600 s, where the updraft is present, is called the early developing stage. In our simulations, prescribed flow is the summation of the updraft and the HIT snapshot.

Table 2 shows the initial temperature and water vapor profiles in the KiD warm1. In the simulations, the temperature field does not change with time, while the water vapor mixing ratio is convected by the updraft. Due to the vertical profile of the KiD warm1, the cloud base is formed around $z = 600$ m and the cloud top is formed around $z = 2000$ m.

Case configurations

In the present study, two cases of simulations named LAM-case and TURB-case are performed. LAM-case stands for laminar case and is the simulation without the HIT snapshot. TURB-case stands for turbulent case and is the simulation with the snapshot. The domain size $L_x^2 \times L_z$ for both simulations is $5^2\ \mathrm{mm}^2 \times 2250$ m. The duration time is 1800 s in both cases. Table 3 shows the computational settings for the two cases.

RESULTS AND DISCUSSION

Figure 3 shows the collision frequency of droplet pairs with the diameter ratio between 1 and 2. Figure 3a shows the collision frequency in LAM-case, while Figure 3b shows that in TURB-case. During the early developing stage ($t < 600$ s), where the updraft is present, there is an exact discrepancy between LAM-case and TURB-case. In LAM-case, the frequency is extremely low in the inner cloud. In TURB-case, on the other hand, the high frequency over $1.0 \times 10^5\ \mathrm{m^{-3}s^{-1}}$ is observed in the inner cloud. This discrepancy indicates that the turbulence promoted the collisions between droplets of simi-

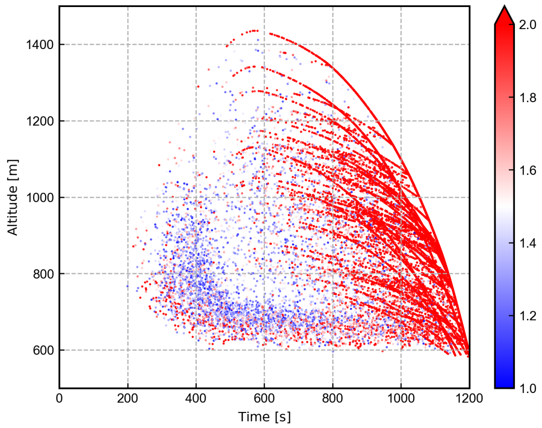

(a) LAM-case.

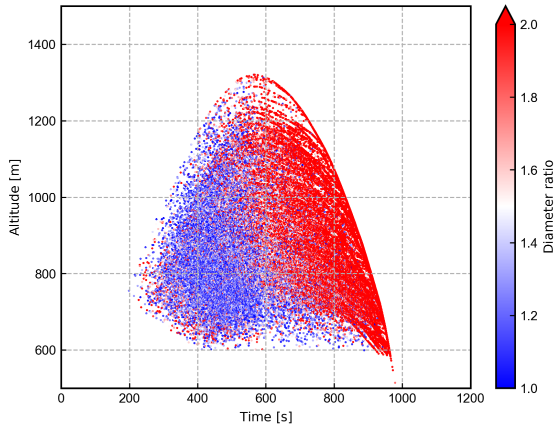

(b) TURB-case.

Figure 5: All collision events of the first surface-reaching raindrops.

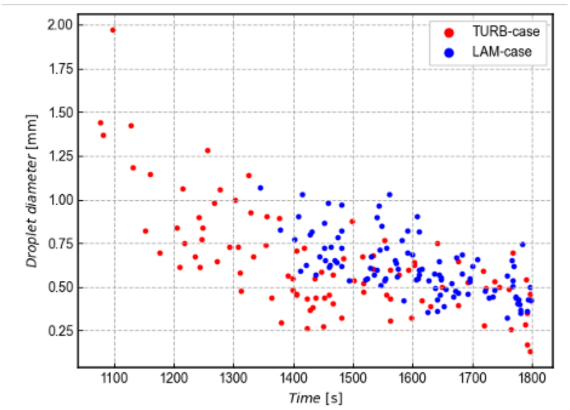

(a) All surface-reaching raindrops in 1800 s simulations.

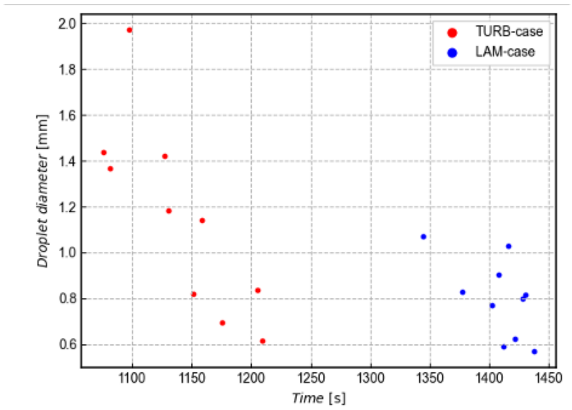

(b) The first 10 surface-reaching raindrops.

Figure 6: The diameter of surface-reaching raindrops against the time they reach the ground.

lar sizes (autoconversions) in the inner cloud during the early stage.

Figure 4 shows the collision frequency of droplet pairs with the diameter ratio of 2 or greater. Figure 4a shows the collision frequency in LAM-case, while Figure 4b shows that in TURB-case. In both cases, high frequency areas over 1.0×10^5 $m^{-3}s^{-1}$ are found after the early developing stage. However, in TURB-case, the area is located around 300 s earlier than in LAM-case. This difference in time is due to the autoconversions promoted by turbulence. The promoted autoconversions generated the relatively large droplets in the inner cloud during the early stage. These large droplets actively collect smaller droplets (accretions). This leads to the earlier location of high collision frequency areas with the diameter ratio of 2 or greater.

Figure 5 shows the all collision events for first surface-reaching raindrop in LAM-case (5a) and TURB-case (5b). The surface-reaching raindrop means the raindrop that reaches the ground surface. Each scatter reveals the collision event of droplet pairs. The color of the scatter shows the diameter ratio of the droplet pairs. In TURB-case, a lot of blue plots, which mean the low diameter ratios, can be found before 600 s. This result indicates that the turbulence promoted autoconversions. In both cases, red plots, which mean the high diameter ratios, are seen after 600 s. However, much more dense red plots are observed in TURB-case than LAM-case. This indicates that relatively large droplets generated by autoconversions before 600 s made active accretions after 600 s. These scenarios are consistent with the analysis of collision frequency shown in Fig 3 and 4.

Figure 6 shows the diameter of surface-reaching raindrops against the time they reach the ground. Figure 6a contains all surface-reaching raindrops in 1800 s of the simulations, while Figure 6b contains only the first 10 surface-reaching raindrops. From the two figures, it is found in TURB-case that the precipitation onset at the ground (the first plot for both simulations) is about 270 s earlier than that in LAM-case. Moreover, the size of raindrops in TURB-case are larger, compared to LAM-case. This trend is particularly pronounced for the first 10 surface-reaching raindrops. The average diameter of the first 10 surface-reaching raindrops in TURB-case is about 1.5 times larger than that in LAM-case. The results depict that the turbulence advances the precipitation onset at the ground and makes surface-reaching raindrops larger just after the precipitation onset.

CONCLUSIONS

We developed a new cloud microphysical model based on direct numerical simulation (DNS) with Lagrangian particle tracking. The novelty of this model lies in the adoption of a vertically-elongated quasi one dimensional computational domain covering from the cloud top to the ground. This new framework enabled us to evaluate the effect of turbulence on the all warm-cloud microphysical processes explicitly.

Using this new model, two simulation cases named TURB-case and LAM-case (with and without turbulent velocity fluctuations, respectively) were performed. The comparison of two simulation results shows large impacts of turbulence on the cloud microphysics.

The turbulence promoted the collisions of droplets. In TURB-case, at the early developing stage with non-zero vertical velocity ($t < 600$ s), collisions of droplet pairs with the diameter ratio between 1 and 2 are promoted in the inner cloud, compared to LAM-case. This indicated that the turbulence promoted the collisions of droplets with similar sizes (autoconversions) in the inner cloud. After the early stage, in both cases, the high collision frequency with the diameter ratio of 2 or greater were found. However, in TURB-case, the area of high collision frequency appeared around 300 s earlier than that in LAM-case. This indicates that the collection of small droplets by relatively large droplets (accretions) is more prominent in TURB-case, compared to LAM-case. These active accretions were induced by the relatively large droplets created by the promoted autoconversions in the early stage. These scenarios were also found in the analysis of all collision events for the first raindrop reaching the ground surface (surface-reaching raindrops).

The turbulence also affects the properties of surface-reaching raindrops. In TURB-case, the onset of precipitation becomes about 270 s earlier than that in LAM-case. Furthermore, in TURB-case, the size of the surface-reaching raindrops is larger, compared to LAM-case. This trend is particularly pronounced for the surface-reaching raindrops just after the precipitation onset. These results indicate that the turbulence advances the precipitation onset at the ground and makes surface-reaching raindrops larger just after the precipitation onset.

ACKNOWLEDGMENT

The simulations were performed on the TSUBAME 4.0 supercomputer in Institute of Science Tokyo.

REFERENCES

Kunishima, Y & Onishi, R 2018 Direct lagrangian tracking simulation of droplet gowth in vertically developing cloud. Atmos. Chem. Phys. 18, 16619–16630.

Onishi, R, Matsuda, K & Takahashi, K 2015 Lagrangian tracking simulation of droplet gowth in turbulence-turbulence enhancement of autoconversion rate. J. Atmos. Sci. 72, 2591–2607.

Saito, I & Gotoh, T 2018 Turbulence and cloud droplets in cumulus clouds. New J. Phys. 20, 1367–2630.

Shipway, B J & Hill, A A 2012 Diagnosis of systematic differences between multiple parametrizations of warm rain microphysics using a kinematic framework. Q. J. Roy. Meteor. Soc. 138, 2196â 2211.

Vaillancourt, P A & Yau, M K 2000 Review of particle-turbulence interactions and consequences for cloud physics. Bull. Amer. Meteor. Soc. 81, 285–298.

Woittiez, E J P, Jonker, H J J & Portela, L M 2009 On the combination of turbulence and gravity on droplet collisions in clouds: a numerical study. J. Atmos. Sci. 66, 1926–1943.